Beta decay rates for r-process for nuclei near neutron number N=82

Kamales $Kar^{a,1}$ and Soumya Chakravarti^{b,2}

^aSaha Institute of Nuclear Physics, 1/AF Bidhan Nagar, Calcutta 700 064, India

^bDepartment of Physics, California State Polytechnic University, Pomona,

CA 91768, USA

ABSTRACT: For r-process nucleosynthesis the beta decay rates of very neutron-rich

nuclei are important ingredients. We consider the region around the neutron number N=82

and calculate the half-lives and rates for a number of nuclei. Forms for beta strength

functions based on spectral distribution methods are used. The calculated half-lives are

first compared to the observed values and then predictions are made for very neutron-rich

nuclei close to drip line for which no experimental values are available.

PACS: 23.40.-s; 26.30.Hj

Keywords: r-process; β decay halflives & rates; Gamow-Teller strength; waiting point

nuclei

1. Introduction

The production of elements heavier than iron takes place through the s-process and r-

process nucleosynthesis [1]. Though roughly half the nuclei with A > 56 are created through

the r-process, its sites are still uncertain. Many candidates have been proposed and the most

¹ Email: kamales.kar@saha.ac.in Tel: (91) 33 2337 5345 FAX: (91) 33 2337 4637

²Email: chakra@csupomona.edu

1

favored ones are all connected to core collapse supernovae. But they have the drawback that the mechanism of explosion of these supernovae is not completely understood yet and almost all simulations with realistic physics input fail to reproduce the explosion [2]. The neutrino driven wind outside a protoneutron star for a delayed core-collapse supernova (DCCSN) is considered to be a promising site. In the environments of high temperatures (a few times 10^9 K) and high neutron density (> 10^{20} cm⁻³) and high entropy, neutron capture is rapid compared to the lifetime of beta decay. So normally a succession of neutron captures takes place followed by a waiting point and then a beta decay. The waiting point is dominant near shell closures. So through r-process nucleosynthesis often very neutron-rich nuclei far away from the valley of stability are produced. As the r-process path goes through the magic nuclei with N=50, 82 and 126, these nuclei can clearly be identified by the observed nuclear abundance peaks [1]. Because of the uncertainties of the sites, a number of site free parametric high temperature r-process models proposed over the years, like the canonical r-process model (CAR) [3], the multi-event r-process model (MER) [4] [5] etc., are quite useful. Over the last two decades radioactive ion beams have been extensively used to create many of the nuclei in the possible r-process path. But some of the nuclei near the drip line are so neutron rich it is difficult to make any detailed measurement in the laboratory. So the knowledge of the nuclear properties of these very large number of nuclei is still far from complete. The nuclear physics of the r-process for these nuclei needs information on ground state properties, (n, γ) and (γ, n) rates, β^- half-lives, beta-delayed neutron emission and different modes of fission. In the absence of experimental data results of theoretical calculations are very useful. Though one prefers microscopic models one expects them to be universal. So theoretical models applicable globally or at least over a region of nuclear masses are of particular relevance. Takahashi and Yokoi [6] calculated beta decay rates for heavy nuclides (25 < Z < 84 and 58 < A < 210) at temperatures 5 \times 10³ < T < 5 \times 10⁷ K and electron density 10²⁰ < n_e < 3 \times 10²⁷cm⁻³. Though this is for all nuclei going through beta decay and electron capture in the s-process paths the method is very general and has wider applicability. They estimate unknown ft-values from sytematics.

Calculation of beta decay and electron capture rates has been pursued vigorously during the last twenty years for pre-supernova evolution and gravitational collapse stage for core collapse supernovae [7]. Whereas for the sd-shell nuclei the rates are given by Oda et al. [8], for the fp-shell nuclei the works of Fuller, Fowler and Newman [9] [10] [11] were used as the standard reference for quite some time. Aufderheide [12] [13] indicated the usefulness of interacting shell model for the rates. They also calculated approximate abundances in stellar conditions appropriate for the pre-supernova and collapse stage and identified the nuclei which are the most important in the network for each density-temperature grid point. On the other hand statistical methods for the beta decay strength distribution were used to calculate the rates for fp-shell nuclei [14]. This was followed by large space and detailed shell model calculations of the allowed beta decay strength to calculate weak interaction rates for nuclei with A < 65 [7] [15]. The effect of the new shell model rates on the late stage of evolution of massive stars has also been seen [16]. Recently Pruet and Fuller [17] used FFN-type ideas supplemented by experimental information wherever available to calculate the rates for nuclei in the mass range A = 65 - 80 relevant for supernova collapse.

There are two classes of models for calculation of beta decay half-lives and rates for neutron rich nuclei. Among the macroscopic models the Gross Theory of beta decay [18] [19]

[20] [21] is one of the earliest models that took into account the Gamow-Teller (GT) giant resonances in some form for nuclei far away from stability. The later improvements [22] [23] known as Semi-Gross Theory or 2nd generation Gross Theory are used for r-process calculations [2]. Among the microscopic approaches to estimate half-lives of a large set of nuclei different versions of a combination of global mass models and Quasiparticle Random Phase Approximation (QRPA) have been used. These are FRDM/QRPA [24] and ETSI/QRPA [25]. Self-consistent Hartree-Fock-Bogoliubov plus QRPA model has also been used [26]. The shell closure at N=82 for n-rich nuclei in the r-process path is receiving a lot of attention lately and more realistic models for beta decay half-lives and rates in this region are needed now. We construct here a model for the beta decay strength function based on the experience with lighter nuclei in the fp shell. This takes into account the tail of the GT giant resonance with the centroid of the resonace empirically fixed and its width obtained by best fit to the known neutron-rich nuclei. We deal with nuclei for which a few lowlying log ft's are known, to test the model and then also apply it to cases where not much is known experimentally beyond the Q-value and half-life. We then use it to predict the experimentally unknown half-lives of nuclei near the drip line where very little data are available. These nuclei may play important roles in the r-process. The actual beta decay rates are also calculated for stellar density and temperatures which are thought to be typical for the r-process. Section 2 describes the model that we construct to calculate the half-lives and rates and section 3 gives the results for such calculations for the neutron-rich nuclei in the mass range of 115 < A < 140.

2. Model For Beta Strength Function

In stellar situations the beta decay of a nucleus, in principle, can take place not only from the ground state of the mother but from the low-lying excited states as well. The contributions from the excited states depend on the temperature. Thus the beta decay rate for a nucleus at temperature T is given by

$$\lambda = \sum_{i} e^{-E_i/kT} \sum_{j} \lambda_{ij}/Z \tag{1}$$

where E_i is the energy of the state of the mother nucleus $|i\rangle$ and Z is the partition function of the nucleus. 'j' sums over final states of the daughter nucleus $|j\rangle$ to which transitions are possible and λ_{ij} stands for the rate between these two states. For allowed decay this rate is given by

$$\lambda_{ij} = \frac{\ln 2}{(ft)_{ij}} f_{ij} = \ln 2 f_{ij} \left[\frac{|M_F|^2}{10^{3.79}} + \frac{|M_{GT}|^2}{10^{3.59}} \right]$$
 (2)

In eq (2) the first part in the brackets is the contribution from the Fermi operator and the second part from the Gamow-Teller operator. Also f_{ij} is the phase space factor for the beta decay with the emitted electron with energy E and rest mass energy $m_e c^2$ going to the top of the electron Fermi sea outside and has the expression

$$f_{ij} = \int_1^{\epsilon_0} F(Z, \epsilon) (\epsilon_0 - \epsilon)^2 \epsilon (\epsilon^2 - 1)^{1/2} (1 - f_e) d\epsilon$$
(3)

with $\epsilon_0 = E_{ij}/m_e c^2$ and $\epsilon = E/m_e c^2$ where E_{ij} is the maximum energy the electron can have for the transition from the state |i> to the state |j>. f_e is the Fermi-Dirac distribution of the electrons outside the nucleus at temperature T. For the antineutrinos under consideration, there is no buildup of antineutrino gas outside. Here $F(Z,\epsilon)$ is the Coulomb correction factor and we use the expression of [27]. In eq (2) the Fermi and the Gamow-Teller matrix elements for $\beta^{-/+}$ decay are given by

$$|M_F(fi)|^2 = |\langle f|\Sigma_k t_{-/+}(k)|i\rangle|^2/(2J_i + 1)$$
(4)

$$|M_{GT}(fi)|^2 = |\langle f|\Sigma_k \vec{\sigma}(k)t_{-/+}(k)|i\rangle|^2/(2J_i+1)$$
(5)

For calculation of half-lives the decay is from the ground state, *i.e.*, there is only one mother state and the Boltzmann factor is equal to 1 in eq (1).

The beta decay strength distribution has contributions from a number of discrete low-lying states of the daughter and the GT giant resonance. However the Fermi resonance is a very sharp one and centred around the Isobaric Analog State (IAS), which gets pushed up in energy above the ground state of the mother by the Coulomb interaction. In our model we take the resonance width as $\sigma_c = 0.157ZA^{-1/3}$ [14] [28]. As the spreading width is small this resonance cannot be reached by Q-value and so Fermi makes very little contribution to half-lives and rates.

However the GT giant resonance is a broad one due to the spin dependence of the Hamiltonian and the GT operator and the tail of the giant resonance can be reached by the Q value. Spectral distribution theory suggests that for a large number of valence nucleons and for very large shell model spaces, the strength distribution in final energy for one-body and similar excitation operators asymptotically goes towards a Gaussian [29] [30]. But the actual GT strength distribution for nuclei often deviate substantially from Gaussian

particularly in the tail region. However in this work we shall take the form of the beta strength coming from the GT giant resonance to be a Gaussian. For the low-lying states of the daughter whose $\log ft$'s are known we explicitly take into account these strengths in the summation of eq (1). Their strengths are subtracted from the GT sum rule strength used for the giant resonance, viz. 3(N-Z), where N and Z are the neutron and proton numbers of the mother. This expression is known as the Ikeda sum expression [31] and normally gives the difference of the β^- and the β^+ strengths. But for our cases as the allowed neutron orbitals for the valence protons are blocked the β^+ sum rule strength is negligibly small. For the GT centroid, Bertsch and Esbensen [32] using the Tamm-Dancoff Approximation give the following expression [17]

$$E_{GT^{-}} = E_{IAS} + \Delta E_{s.o.} + 2[k_{\sigma\tau}S_{GT^{-}}/3 - (N-Z)k_{\tau}]$$
(6)

where $\Delta E_{s.o.}$ is the contribution coming from the spin-orbit force. and we use the orbit averaged value of 3.0 MeV [32] for it. The last two terms have their origin in the spin-isospin and isospin dependent nuclear forces. Like Pruet and Fuller [17] we use the values $k_{\tau} = 28.5/A$ and $k_{\sigma\tau} = 23/A$. It is wellknown that the actual GT strength sums are quenched compared to the theoretical values. We take this into account by an overall quenching factor of 0.6 in the sum rule [14]. The width of the Gaussian is left as a free parameter to best reproduce the half-lives of decaying nuclei in the range 115 < A < 140. The β^- decays with Q values greater than 5 MeV are selected as one needs enough final states to use the statistical averaged strength function. Decays with lower Q values are normally dominated by specific transitions to one or two states and for them microscopic

models are required. The nuclei in this range are divided into two groups: i) nuclei for which some low-lying $\log ft$'s are known, and ii) nuclei for which no measured low-lying $\log ft$ is available. The second group of nuclei are the more neutron rich ones and on the average have larger Q values. As the r-process nuclei roughly have Q values of 10 MeV or more, again the second group are the ones that are more relevant for r-process. The width extracted for the second group is the one that can be used for the prediction of half-lives of nuclei near the drip-line taking part in the r-process. This is done for a number of isotopes in this mass range for which very little experimental information is available.

We also observe that for odd-N nuclei with N > 82, as the neutrons and protons occupy different shells, the parity of the ground state of the mother is different from the parity of the states in the ground state region of the daughter. So there are normally no allowed transitions from the ground state of the mother to the low-lying states of the daughter and instead one has much weaker transitions coming from the forbidden beta decays. The GT transitions take place to states at higher energies and our model can handle that situation too.

3. Results

We first consider the set of nuclei in the mass range of 115 to 140 for which some low-lying $\log ft$ values are known [34]. The width of the Gamow Teller resonance is varied to minimise the quantity $S = \sum_n [\log \left(\tau_{1/2,\mathrm{calc}}/\tau_{1/2,\mathrm{expt}}\right)]^2$ summed over all the n=32 nuclei. Table 1 gives the calculated values of the half-lives and compares them with the experimental values [34]. The best fit value of the width is 4.2 MeV and for that width S/n turns out to be 0.2630.

One finds that 20 of the calculated values are within a factor of 2 from the experimental half-lives while 9 more are within a factor of 5. Only the nuclei 119 Ag, 122 In and 123 Ag have their calculated values off by factors of ten or more and all three have the experimental values much smaller. Excluding them the value of S/n turns out to be 0.0744. Excluding only 122 In and 123 Ag makes it 0.1088.

Table 2 gives the calculated and experimental half-lives for 37 nuclei in the same mass range. The best fit value for the GT width is 6.9 MeV. The value for S/n in this case is 0.1131. 23 of the calculated half-lives are within a factor of 2 from the observed values and the remaining 14 are all within a factor 5. The value of the width turns out to be larger than the GT giant resonance width. However we point out that in our model, the resonance has been artificially made wider to take account of some of the discrete strengths to states lying below the giant resonance. Figure 1 shows the cases without known $\log ft$'s alongwith the cases with the known ones, i.e., 69 cases in all with the value of $\log \left(\tau_{1/2,\text{calc}}/\tau_{1/2,\text{expt}}\right)$ plotted as a function of the Q value. In Figure 2 we plot the calculated half-lives of all the 69 nuclei and compare them with a simple form which depends only on the Q value given by

$$\lambda_{\beta^{-}} = \ln 2/t_{1/2} = 10^{-4} \times (Q_{\beta^{-}}/MeV)^5 \ s^{-1}$$
 (7)

This form in a log-log plot is a straight line and represents the case where the GT matrix element has a fixed value independent of energy [2]. We particularly mention two important waiting point nuclei ¹²⁹Ag and ¹³⁰Cd. For ¹²⁹Ag our prediction is 0.124 s compared to the experimental half-life of 0.046 s, whereas the earlier prediction of RPA calculations was 0.172 s. Similarly for ¹³⁰Cd our calculation gives the half-life as 0.294 s with the experimental

value as 0.162 s and the earlier prediction was 0.195 s [33].

After demonstrating that the model for beta strength distribution works well we use this for predicting half-lives of the very neutron-rich nuclei for which the experimental data are not available and which are in the r-process path. Table 3 gives the predicted half-lives for 25 such nuclei. These are nuclei considered to estimate the nuclear shell effects at N = 82 in the r-process region [35].

Finally Table 4 shows the beta decay rates calculated for two typical nuclei ¹³⁰Ag and 126 Ru. For the first nucleus the half-life is known but not the log ft to specific states, and for the second even the half-life is not known. The rates are calculated for a large grid of temperature and density. The temperatures are taken in the range of 0.5 to 8×10^9 K and the density in the range of 10^3 to 10^9 g/cc. As the density increases the chemical potential of the electrons goes up making fewer beta decays energetically possible. The temperature dependence is seen to be very mild coming from the phase space integral of the electrons. It should be mentioned here that the rates are calculated for transitions only from the ground state of the mother. However for large enough temperatures some of the odd-odd nuclei having low-lying states may have contributions from a few excited states also. But for most of the neutron-rich nuclei of interest, there are no observed excitation spectra and one has to use a statistical method to take into account the contributions from the excited states of the mother. The departure from a Gaussian shape can also be taken into account by including effects of higher moments in a parametric form. The so-called 'back resonances' of some special excited states with large overlap with the daughter ground state region are also important for the higher temperatures and need to be taken into account. The model

also needs to be extended to higher masses.

After this work was completed we came to know of the paper by Cuenca-Garcia et al. [36], wherein results of large-scale shell model calculations of the half-lives of r-process waiting point nuclei at N=82 are presented. A detailed comparison of this work with ours will also be included in a future work.

References

- [1] E.M. Burbidge, G.R. Burbidge, W.A. Fowler and F. Hoyle, Rev. Mod. Phys. 29 (1957) 547
- [2] M. Arnould, S. Goriely and K. Takahashi, Phys. Rep. 450 (2007) 97
- [3] P.A. Seeger, W.A. Fowler and D.D. Clayton, Astrophys. J. 11 (Suppl.) (1965) 121
- [4] S. Goriely and M. Arnould, Astron. Astrophys. **312** (1996) 327
- [5] V. Bouquelle, N. Cerf, M. Arnould et al., Astron. Astrophys. 305 (1995) 1005
- [6] K. Takahashi and K. Yokoi, Atomic Data and Nucl. Data Tables 36 (1987) 375
- [7] K. Langanke and G. Martinez-Pinedo, Rev. Mod. Phys. 75 (2003) 819
- [8] T. Oda, M. Hino, K. Muto, M. Takahara and K. Sato, At. Data and Nuc. Data Tables 56 (1994) 231
- [9] G.M. Fuller, W.A. Fowler and M.J. Newman, Astrophys. J. S. 42 (1980) 447 (FFN I)
- [10] G.M. Fuller, W.A. Fowler and M.J. Newman, Astrophys. J. S. 48 (1982a) 279 (FFN III)
- [11] G.M. Fuller, W.A. Fowler and M.J. Newman, Astrophys. J. 252 (1982b) 715 (FFN II)
- [12] M.B. Aufderheide, Nucl. Phys. A **526** (1991) 161
- [13] M.B. Aufderheide, I. Fushiki, S.E. Woosley and D.H. Hartmann, Astrophys. J. 91 (1994) 389
- [14] K. Kar, A. Ray and S. Sarkar, Astrophys. J. 434 (1994) 662

- [15] K. Langanke and G. Martinez-Pinedo, Atom. Data and Nuc. Data Tables 79 (2001) 1
- [16] A. Heger, S.E. Woosley, G. Martinez-Pinedo and K. Langanke, Astrophys. J. 560 (2001) 307
- [17] J. Pruet and G.M. Fuller, Astrophys. J. S. 149 (2003) 189
- [18] M. Yamada, Bull. Sci. Eng. Res. Lab. Waseda Uni. (No. 32) (1965) 146
- [19] K. Takahashi and M. Yamada, Prog. Theor. Phys. 41 (1969) 1470
- [20] K.Yako, H. Sakai, M.B. Greenfield et al. Phys. Lett. **B 615** (2005) 193
- [21] K. Takahashi, Prog. Theor. Phys. 45 (1971) 1466
- [22] T. Tachibana, M. Yamada and Y. Yoshida, Prog. Theor. Phys. 84 (1990) 641
- [23] H. Nakata, T. Tachibana and M. Yamada, Nucl. Phys. A 625 (1997) 521
- [24] P. Moller, J.R. Nix and K.L. Kratz, At. Data and Nuc. Data Tables, 66 (1997) 131
- [25] I. Borzov and S. Goriely, Phys. Rec. C 62 (2000) 035501
- [26] J. Engel, M. Bender, J. Dobaczewski, W. Nazarewicz and R. Surman, Phys. Rev. C 60 (1999) 014302
- [27] G.K. Schenter and P. Vogel, Nucl. Sci. Eng. 83 (1983) 393
- [28] M. Morita, Beta Decay and Muon Capture (W.A. Benjamin, USA, 1973)
- [29] J.B. French, V.K.B. Kota, A. Pandey and S. Tomosovic, Ann. Phys. (N.Y.) 181 (1988) 235
- [30] V.K.B. Kota and K.Kar, Pramana J. Phys. **32** (1989) 647
- [31] K. Ikeda, S. Fujii and J.I. Fujita, Phys. Lett. 3 (1963) 271
- [32] G.F. Bertsch and H. Esbensen, Rep. Prog. Phys. **50** (1987) 607
- [33] K.-L. Kratz et al., Z. Phys. A 325 (1986) 489
- [34] R.B. Firestone, Table of Isotopes (V.S. Shirley ed.) (John Wiley, 1996)
- [35] A.R. Farhan and M.M. Sharma, Phys. Rev. C 73 (2006) 045803
- [36] J.J. Cuenca-Garcia, G. Martinez-Pinedo, K. Langanke, F. Nowacki, and I.N. Borzov, Eur. Phys. J., A 34 (2007) 99

Table 1. Half-lives of nuclei for which $\log ft$ values are available and were used.

	Mother	Daughter	Q-value	No of lowlying	$ au_{1/2}$	$ au_{1/2}$
	nucleus	nucleus		$\log ft$'s taken	Expt	Calc
			(MeV)		(sec)	(sec)
1.	$^{116}_{45}\mathrm{Rh}_{71}$	$^{116}\mathrm{Pd}$	8.900	3	0.680	0.496
2.	$^{116}_{47}\mathrm{Ag}_{69}$	$^{116}\mathrm{Cd}$	6.160	5	160.8	162.8
3.	$^{118}_{47}\mathrm{Ag}_{71}$	$^{118}\mathrm{Cd}$	7.060	4	3.76	7.61
4.	$^{119}_{47}\mathrm{Ag}_{72}$	$^{119}\mathrm{Cd}$	5.350	3	2.1	23.61
5.	$^{120}_{47}\mathrm{Ag}_{73}$	$^{120}\mathrm{Cd}$	8.2	4	1.23	0.573
6.	$^{120}_{49}\mathrm{In}_{71}$	$^{120}\mathrm{Sn}$	5.370	3	3.08	2.90
7.	$^{121}_{47}\mathrm{Ag}_{74}$	$^{121}\mathrm{Cd}$	6.400	4	0.78	2.42
8.	$^{122}_{47}\mathrm{Ag}_{75}$	$^{122}\mathrm{Cd}$	9.1	4	0.48	0.393
9.	$^{122}_{49}\mathrm{In}_{73}$	$^{122}\mathrm{Sn}$	6.370	3	1.5	59.30
10.	$^{123}_{47}\mathrm{Ag}_{76}$	$^{123}\mathrm{Cd}$	7.400	5	0.309	12.69
11.	$^{123}_{48}\mathrm{Cd}_{75}$	$^{123}\mathrm{In}$	6.120	3	2.10	9.46
12.	$^{124}_{49}\mathrm{In}_{75}$	$^{124}\mathrm{Cd}$	7.36	3	3.17	6.60
13.	$^{125}_{48}\mathrm{Cd}_{77}$	$^{125}\mathrm{In}$	7.16	4	0.65	1.32
14.	$^{125}_{49}\mathrm{In}_{76}$	$^{125}\mathrm{Sn}$	5.418	6	2.36	2.93
15.	$^{126}_{49}\mathrm{In}_{77}$	$^{126}\mathrm{Sn}$	8.210	4	1.60	2.45
16.	$^{127}_{49}\mathrm{In}_{78}$	$^{127}\mathrm{Sn}$	6.510	4	1.09	1.23
17.	$^{128}_{48}\mathrm{Cd}_{80}$	$^{128}\mathrm{In}$	7.100	4	0.34	0.248

Table 1 (contd.)

	Mother	Daughter	Q-value	No of lowlying	$ au_{1/2}$	$ au_{1/2}$
	nucleus	nucleus		$\log ft$'s taken	Expt	Calc
			(MeV)		(sec)	(sec)
18.	$^{128}_{49}\mathrm{In}_{79}$	$^{128}\mathrm{Sn}$	8,980	3	0.84	2.28
19.	$^{129}_{49}\mathrm{In}_{80}$	$^{129}\mathrm{Sn}$	7.660	2	0.61	0.664
20.	$^{130}_{49}\mathrm{In}_{81}$	$^{130}\mathrm{Sn}$	10.250	2	0.32	0.265
21.	$^{131}_{49}\mathrm{In}_{82}$	$^{131}\mathrm{Sn}$	9.180	3	0.282	0.273
22.	$^{132}_{49}\mathrm{In}_{83}$	$^{132}\mathrm{Sn}$	13.600	4	0.201	0.166
23.	$^{132}_{51}{ m Sb}_{81}$	$^{132}\mathrm{Te}$	5.290	5	167.4	136.6
24.	$_{50}^{133}\mathrm{Sn}_{83}$	$^{133}\mathrm{Sb}$	7.830	2	1.44	1.18
25.	$^{135}_{52}\mathrm{Te}_{83}$	$^{135}\mathrm{In}$	5.960	3	19.0	19.2
26.	$^{136}_{52}\mathrm{Te}_{84}$	$^{136}\mathrm{I}$	5.070	4	17.5	26.8
27.	$^{136}_{53}\mathrm{I}_{83}$	$^{136}\mathrm{Xe}$	6.930	3	83.4	91.8
28.	$^{137}_{53}\mathrm{I}_{84}$	$^{137}\mathrm{Xe}$	5.880	2	24.5	50.4
29.	$^{138}_{53}\mathrm{I}_{85}$	$^{138}\mathrm{Xe}$	7.820	3	6.49	9.57
30.	$^{138}_{55}\mathrm{Cs}_{83}$	$^{138}\mathrm{Ba}$	5.373	3	2004.6	506.9
31.	$^{139}_{54}\mathrm{Xe}_{85}$	$^{139}\mathrm{Ba}$	5.057	6	39.68	70.06
32.	$^{140}_{55}\mathrm{Cs}_{85}$	$^{140}\mathrm{Ba}$	6.219	5	63.7	94.8

Table 2. Half-lives of nuclei for which no $\log ft$ values are available

	Mother	Daughter	Q-value	$ au_{1/2}$	$ au_{1/2}$
	nucleus	nucleus		Expt	Calc
			(MeV)	(sec)	(sec)
1.	$^{116}_{43}\mathrm{Tc}_{73}$	$^{116}\mathrm{Ru}$	11.6	0.09	0.111
2.	$^{116}_{44}\mathrm{Ru}_{72}$	$^{116}\mathrm{Rh}$	6.3	0.4	0.977
3.	$^{117}_{43}\mathrm{Tc}_{74}$	$^{117}\mathrm{Ru}$	10.1	0.04	0.144
4.	$^{117}_{44}\mathrm{Ru}_{73}$	$^{117}\mathrm{Rh}$	8.9	0.3	0.217
5.	$^{117}_{45}\mathrm{Rh}_{72}$	$^{117}\mathrm{Pd}$	7.000	0.44	0.737
6.	$^{117}_{46}\mathrm{Pd}_{71}$	$^{117}\mathrm{Ag}$	5.700	4.3	2.08
7.	$^{118}_{45}\mathrm{Rh}_{73}$	$^{118}\mathrm{Pd}$	10.4	0.3	0.194
8.	$^{119}_{46}\mathrm{Pd}_{73}$	$^{119}\mathrm{Ag}$	6.500	0.92	1.04
9.	$^{120}_{46}\mathrm{Pd}_{74}$	$^{120}\mathrm{Ag}$	5.55	0.5	1.85
10.	$^{122}_{45}\mathrm{Rh}_{77}$	$^{122}\mathrm{Pd}$	11.8	0.05	0.107
11.	$^{124}_{46}\mathrm{Pd}_{78}$	$^{124}\mathrm{Ag}$	7,7	0.2	0.383
12.	$^{124}_{47}\mathrm{Ag}_{77}$	$^{124}\mathrm{Cd}$	10.21	0.172	0.200
13.	$^{125}_{47}\mathrm{Ag}_{78}$	$^{125}\mathrm{Cd}$	8.56	0.188	0.307
14.	$^{126}_{47}\mathrm{Ag}_{79}$	$^{126}\mathrm{Cd}$	11.33	0.107	0.135
15.	$^{126}_{48}\mathrm{Cd}_{78}$	$^{126}\mathrm{In}$	5.490	0.506	1.86
16.	$^{127}_{47}\mathrm{Ag}_{80}$	$^{127}\mathrm{Cd}$	9.62	0.79	0.170
17.	$^{127}_{48}\mathrm{Cd}_{79}$	$^{127}\mathrm{In}$	8,470	0.43	0.338
18.	$^{128}_{47}\mathrm{Ag}_{81}$	$^{128}\mathrm{Cd}$	12.5	0.058	0.0961
19.	$^{129}_{47}\mathrm{Ag}_{82}$	$^{129}\mathrm{Cd}$	10.7	0.046	0.124

Table 2 (cont.)

	Mother	Daughter	Q-value	$ au_{1/2}$	$ au_{1/2}$
	nucleus	nucleus		Expt	Calc
			(MeV)	(sec)	(sec)
20.	$^{129}_{48}\mathrm{Cd}_{81}$	$^{129}\mathrm{In}$	9.74	0.29	0.194
21.	$^{130}_{47}\mathrm{Ag}_{83}$	$^{130}\mathrm{Cd}$	15.4	0.050	0.0627
22.	$^{130}_{48}\mathrm{Cd}_{82}$	$^{130}\mathrm{In}$	8.29	0.162	0.294
23.	$^{131}_{48}\mathrm{Cd}_{83}$	$^{131}{ m In}$	12.84	0.068	0.0923
24.	$^{132}_{48}\mathrm{Cd}_{84}$	$^{132}\mathrm{In}$	19.19	0.097	0.0598
25.	$^{133}_{49}\mathrm{In}_{84}$	$^{133}\mathrm{Sn}$	13.0	0.180	0.0970
26.	$^{134}_{49}\mathrm{In}_{85}$	$^{134}\mathrm{Sn}$	14.85	0.140	0.0767
27.	$^{134}_{50}\mathrm{Sn}_{84}$	$^{134}\mathrm{Sb}$	6.800	1.04	0.664
28.	$^{134}_{51}{ m Sb}_{83}$	$^{134}\mathrm{Te}$	8.420	0.85	0.386
29.	$^{135}_{49}\mathrm{In}_{86}$	$^{135}\mathrm{Sn}$	13.6	0.092	0.0795
30.	$^{135}_{50}\mathrm{Sn}_{85}$	$^{135}\mathrm{Sb}$	8.9	0.530	0.249
31.	$^{135}_{51}\mathrm{Sb}_{84}$	$^{135}\mathrm{Te}$	8.120	1.71	0.403
32.	$^{136}_{50}\mathrm{Sn}_{86}$	$^{136}\mathrm{Sb}$	8.4	0.25	0.279
33.	$^{136}_{51}{ m Sb}_{85}$	$^{136}\mathrm{Te}$	9.3	0.82	0.250
34.	$^{137}_{50}\mathrm{Sn}_{87}$	$^{137}\mathrm{Sb}$	10.0	0.190	0.158
35.	$^{137}_{52}\mathrm{Te}_{85}$	$^{137}\mathrm{I}$	6.940	2.495	0.670
36.	$^{138}_{62}\mathrm{Te}_{86}$	$^{138}\mathrm{I}$	6.370	1.4	0.948
37.	$^{139}_{53}\mathrm{I}_{86}$	$^{139}\mathrm{Xe}$	6.806	2.29	0.691

Table 3. Predicted half-lives for very neutron-rich nuclei (Q values are from [34])

	Mother	Daughter	Q-value	Predicted
	nucleus	nucleus		$ au_{1/2}$
			(MeV)	(sec)
1.	$^{116}_{36}{ m Kr}$	$^{116}_{37}\mathrm{Rb}$	21.30	0.0114
2.	$^{118}_{36}{ m Kr}$	$^{118}_{37}\mathrm{Rb}$	21.76	0.0100
3.	$^{120}_{36}{ m Kr}$	$_{37}^{120}{ m Rb}$	23.55	0.00881
4.	$^{122}_{36}{ m Kr}$	$_{37}^{122}\mathrm{Rb}$	25.71	0.00783
5.	$^{118}_{38}\mathrm{Sr}$	$^{118}_{39}{ m Y}$	18.21	0.0167
6.	$^{120}_{38}{ m Sr}$	$^{120}_{39}{ m Y}$	19.75	0.0141
7.	$^{122}_{38}\mathrm{Sr}$	$^{122}_{39}{ m Y}$	21.55	0.0122
8.	$^{124}_{38}\mathrm{Sr}$	$^{124}_{39}{ m Y}$	22.47	0.0108
9.	$^{120}_{40}{ m Zr}$	$^{120}_{41}{ m Nb}$	14.86	0.0278
10.	$^{122}_{40}{ m Zr}$	$^{122}_{41}{ m Nb}$	16.68	0.0215
11.	$^{124}_{40}{ m Zr}$	$^{124}_{41}{ m Nb}$	18.61	0.0175
12.	$^{126}_{40}{ m Zr}$	$^{126}_{41}{ m Nb}$	19.56	0.0152
13.	$^{122}_{42}{ m Mo}$	$^{122}_{43}{ m Tc}$	11.60	0.0585
14.	$^{124}_{42}{ m Mo}$	$^{124}_{43}{ m Tc}$	13.61	0.0375
15.	$^{126}_{42}{ m Mo}$	$^{126}_{43}{ m Tc}$	12.82	0.0370

Table 3 (contd.)

	Mother	Daughter	Q-value	Predicted
	nucleus	nucleus		$ au_{1/2}$
			(MeV)	(sec)
16.	$^{128}_{42}{ m Mo}$	$^{128}_{43}{ m Tc}$	15.25	0.0249
17.	$^{124}_{44}\mathrm{Ru}$	$^{124}_{45}\mathrm{Rh}$	8.60	0.178
18.	$^{126}_{44}{ m Ru}$	$^{126}_{45}\mathrm{Rh}$	9.94	0.101
19.	$^{128}_{44}{ m Ru}$	$^{128}_{45}\mathrm{Rh}$	11.60	0.0599
20.	$^{130}_{44}\mathrm{Ru}$	$^{130}_{45}\mathrm{Rh}$	16.56	0.0306
21.	$^{126}_{46}{ m Pd}$	$^{126}_{47}\mathrm{Ag}$	8.27	0.2619
22.	$^{128}_{46}{ m Pd}$	$^{128}_{47}\mathrm{Ag}$	10.39	0.1165
23.	$^{130}_{46}{ m Pd}$	$^{130}_{47}\mathrm{Ag}$	12.28	0.07009
24.	$^{132}_{46}{ m Pd}$	$^{132}_{47}\mathrm{Ag}$	16.56	0.04706
25.	$^{134}_{48}Cd$	$^{134}_{49}{ m In}$	11.57	0.09227

Table 4. Beta decay rates for the nuclei $^{126}\mathrm{Ru}$ and $^{130}\mathrm{Ag}$

NUCLEUS	DENSITY			TEMP T ₉		
	(g/cm^3)	0.5	1.0	2.0	4.0	8.0
	10^{9}	3.56	4.29	5.12	4.79	4.22
	10^{8}	6.27	6.29	5.74	4.90	4.24
	10^{7}	6.77	6.49	5.80	4.91	4.24
$^{126}\mathrm{Ru}$	10^{6}	6.80	6.51	5.80	4.91	4.24
	10^{5}	6.80	6.51	5.80	4.91	4.24
	10^{4}	6.80	6.51	5.80	4.91	4.24
	10^{3}	6.80	6.51	5.80	4.91	4.24
	10^{9}	7.44	8.16	8.94	8.24	7.14
	10^{8}	10.43	10.42	9.70	8.39	7.15
	10^{7}	10.93	10.63	9.77	8.41	7.16
$^{130}\mathrm{Ag}$	10^{6}	10.97	10.65	9.78	8.41	7.16
	10^{5}	10.97	10.65	9.78	8.41	7.16
	10^{4}	10.97	10.65	9.78	8.41	7.16
	10^{3}	10.97	10.65	9.78	8.41	7.16

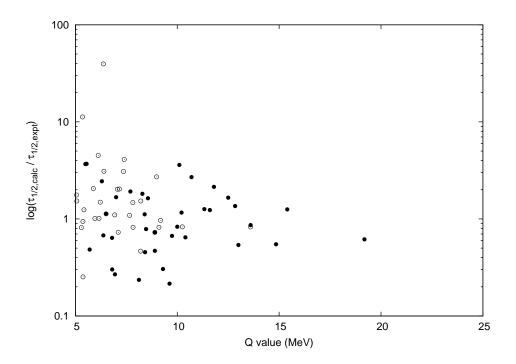


Figure 1: $\log(\tau_{1/2,\text{calc}}/\tau_{1/2,\text{exp}})$ plotted against Q value for 69 nuclei (see text). Results for nuclei with known (unknown) log ft's are shown as open (filled) circles.

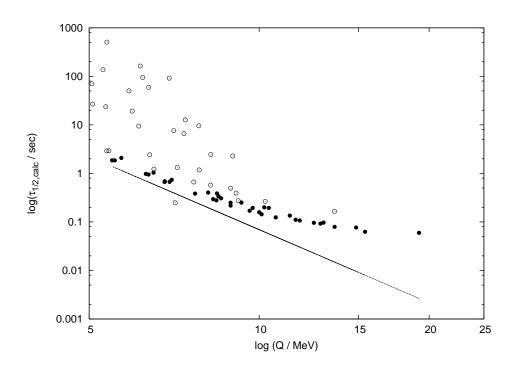


Figure 2: Calculated half-lives of 69 nuclei plotted against Q values in a log-log plot.

Results for nuclei with known (unknown) log ft's are shown as open (filled) circles.

A power law dependence is shown for comparison (see text).